JOURNAL OF CATALYSIS **168,** 315–320 (1997)
ARTICLE NO. CA971662

The Effect of Oxygen-Anion Conductivity of Metal–Oxide Doped Lanthanum Oxide Catalysts on Hydrocarbon Selectivity in the Oxidative Coupling of Methane

Holger Borchert* and Manfred Baerns†

Lehrstuhl für Technische Chemie, Ruhr-Universität Bochum, D-44780 Bochum, Germany

Received June 20, 1996; revised February 5, 1997; accepted February 5, 1997

La_2O_3 was doped with cations of valencies different to La^{3+} (Sr^{2+}, Zn^{2+}, Ti^{4+}, Nb^{5+}) to alter the concentration of oxygen–anion vacancies in the host lattice and, hence, oxygen-anion conductivity. The conductivity and catalytic properties of these solids were determined between 700 and 850°C. An increase in oxygen-anion conductivity improved C_{2+} selectivity. A high concentration of anion vacancies in the catalytic material favours the adsorption of gaseous oxygen and its immediate transformation into lattice oxygen; therefrom it is suggested, that the relative amount of weakly adsorbed electrophilic oxygen species (possibly O_2^-, O_2^{2-}) is diminished in favour of more strongly bounded, nucleophilic species (O^{2-}). Thereby, nonselective surface reactions of methyl radicals and/or C_{2+} hydrocarbons with electrophilic oxygen are suppressed. © 1997 Academic Press

INTRODUCTION

In the oxidative coupling of methane (OCM) to C_2-hydrocarbons the nature of oxygen species participating in the reaction is not yet fully understood. Adsorbed oxygen species of electrophilic character (e.g., O_2^-, O_2^{2-}, O^-), as well as lattice oxygen (O^{2-}), are supposed to be responsible for C–H bond cleavage to produce methyl radicals. The interaction of adsorbed oxygen species with weakly adsorbed or gas-phase methane molecules can directly result in the homolytic formation of a methyl radical (see reaction [1]) (1, 2), while methane activation via highly basic surface lattice oxygen follows a heterolytic cleavage after which the removal of an electron from CH_3^--species is required to generate methyl radicals (see reaction [2]) (3, 4). In addition, electrophilic oxygen species are also involved in the nonselective oxidation of methyl radicals and C_2-hydrocarbons (5):

$$CH_4 + O_x^- \ (x = 1 \text{ or } 2) \Leftrightarrow CH_3^\bullet + HO_x^- \qquad [1]$$

$$\begin{aligned} CH_3{-}H + [M^{n+}O^{2-}] &\Leftrightarrow [M^{n+}OH^-] + CH_3^- \\ &\rightarrow M^{(n-1)+}OH^- + CH_3^\bullet. \end{aligned} \qquad [2]$$

On metal oxide surfaces all these oxygen species might exist in an equilibrium state:

$$O_2(g) \Leftrightarrow O_2(s) \overset{+e}{\Leftrightarrow} O_2^-(s) \overset{+e}{\Leftrightarrow} O_2^{2-}(s) \Leftrightarrow 2\,O^-(s) \overset{+2e}{\Leftrightarrow} 2\,O^{2-}, \qquad [3]$$

depending on oxygen partial pressure, temperature, and the ability of the metal oxide to transform weakly adsorbed oxygen entities into lattice oxygen (6–12). A high surface concentration of oxygen anion vacancies favours oxygen adsorption and transformation into less electrophilic species (O^-, O^{2-}), whereas a low concentration of these defects gives rise to a high concentration of weakly adsorbed, molecular oxygen (O_2^-, O_2^{2-}) by which oxygen insertion to any CH_x-species is favoured which leads to total oxidation. Thus the catalytic properties ought to be dependent on the concentration of vacancies and the mobility of the oxygen-anions as recently reviewed (6).

It has been reported that many selective OCM catalysts have oxygen anion vacancies in the oxide lattice, which lead to the mobility of oxygen anions at temperatures (>700°C) applied in the OCM (7, 13–16).

The oxygen-anion conductivity (σ_{ion}) of metal oxides is related to the concentration of oxygen vacancies $c(V_O^{\bullet\bullet})$, their charge z_e, and their mobility μ_{ion} (17); using the Kroeger–Vink-notation one obtains

$$\sigma_{ion} = c(V_O^{\bullet\bullet}) * 2e * \mu_{ion}; \qquad [4]$$

the mobility further depends on temperature,

$$\mu_{ion} \sim \exp(-E_a/RT), \qquad [5]$$

where E_a denotes the activation energy for the oxygen mobility.

---

*Present address: Hoechst AG, Central Research, D-65926 Frankfurt, Germany.

†Present address: Institute for Applied Chemistry Berlin-Adlershof e.V., Rudower Chaussee 5, D-12484 Berlin, Germany. Correspondence author. E-mail: baerns@aca.fta-berlin.de.

0021-9517/97 $25.00

Besides anionic conductivity most of the selective catalysts exhibit defect electron conductivity (σ_p), which results from the uptake of oxygen which interacts with the anion vacancies (18).

In the present work, La_2O_3 known as OCM catalyst (2, 19, 20), was doped with cations having different valencies (Zn^{2+}, Sr^{2+}, Ti^{4+}, and Nb^{5+}) in order to affect the number of oxygen vacancies in the host lattice. Whereas lower valent dopants (Sr^{2+}, Zn^{2+}) cause the formation of oxygen-anion vacancies, their concentration decreases when doping with cations of higher valency (Ti^{4+}, Nb^{5+}) (6). The total conductivity ($\sigma_{\text{ion}} + \sigma_p$) as well as the oxygen-anion conductivities of such catalysts were determined in the temperature range required for the OCM reaction; the conductivity data were then related to the corresponding C_{2+} selectivities. In interpreting the results it is assumed that the concentration of oxygen anion vacancies in the bulk and on the surface are interrelated by a dynamic equilibrium; i.e., the absolute values may be different in the bulk and on the surface.

METHODS

Catalyst Preparation

La_2O_3 was doped with 1 at-% of Zn^{2+}, Ti^{4+}, and Nb^{5+} and different amounts of Sr^{2+} (0.5, 1.0, 2.0, 3.0, 20.0 at-%) as indicated in Table 1 which also contains further details of the preparation procedure. For the catalytic experiments the calcined pellets were crushed and sieved (0.25–0.35 mm). The specific surface area of the catalysts determined by the BET method was in all cases less than 1 m^2/g (S_{BET}/m^2g^{-1}. La_2O_3 : 0.8; Nb^{5+} (1 at-%)/La_2O_3: 0.8; Ti^{4+} (1 at-%)/La_2O_3: 0.9; Zn^{2+} (1 at-%)/La_2O_3: 0.5; Sr^{2+} (1 at-%)/La_2O_3: 0.8).

TABLE 1

Methods for Catalyst Preparation

Catalyst	Preparation method
La_2O_3	Evaporation of a $La(NO_3)$ aqueous solution to dryness, calcination at 1373 K for 24 h.
Nb^{5+} (1 at-%)/La_2O_3	Mixing of aqueous solutions of niobium oxalate and $La(NO_3)_3 * 6H_2O$, evaporation to dryness, calcination at 1073 K for 12 h followed by 1373 K for 168 h.
Ti^{4+} (1 at-%)/La_2O_3 Zn^{2+} (1 at-%)/La_2O_3 Sr^{2+} (0.5 at-%)/La_2O_3 Sr^{2+} (1 at-%)/La_2O_3	Mechanical mixing of TiO_2, $Zn(NO_3)_2 * 4H_2O$ or $Sr(NO_3)_2$ with La_2O_3, calcination at 1373 K for 24 h.
Sr^{2+} (2 at-%)/La_2O_3 Sr^{2+} (3 at-%)/La_2O_3 Sr^{2+} (20 at-%)/La_2O_3	Evaporation of an aqueous solution of $Sr(NO_3)_2$ and $La(NO_3)_3 * 6H_2O$, calcination at 1073 K for 12 h followed by 1373 K for 168 h.

TABLE 2

Relative Bulk and Surface Composition of Sr_{2+}/La_2O_3 Catalysts

	$Sr^{2+}/(Sr^{2+} + La^{3+})$ (at-%)				
Bulk[a]	0.5	1.0	2.0	3.0	20.0
Surface[b]	7.7	16.5	17.1	n.d.	38.6

[a] According to catalyst preparation.

[b] Measured by XPS.

Characterization of Surface Composition

The surface composition of the SrO/La_2O_3 catalysts was determined by XPS (Leybold Heraeus LHS-10 spectrometer, Al K_α X-ray source); the La $3d_{5/2}$, O 1*s* and Sr 3*d* peaks were used, applying Wagner's sensitivity factors for quantitative analysis. The surface concentration of Sr^{2+} on the SrO/La_2O_3 catalysts are listed in Table 2; for comparison the bulk concentration of Sr is also given.

Catalyst Testing

Catalysts were tested in a catalytic fixed-bed reactor (8 mm i.d.) made of quartz. Good temperature control of the reactor was achieved by immersing it into a fluidized bed of sand serving as a source or a sink of heat. The product gas from which water was removed by condensation was analysed by gas chromatography (21).

The OCM reaction was performed at 973, 1023, 1073, and 1123 K; the feed gas consisted of methane (60 kPa), oxygen (6 kPa), and nitrogen (34 kPa). For comparison of selectivities obtained at different degrees of oxygen or methane conversion, respectively, the dependence of C_{2+} selectivity on oxygen conversion was investigated by varying the modified contact time ($=m_{cat}/V_{T,P}$) from 0.001 to 0.05 $g \cdot s \cdot ml^{-1}$ at 1023 K. When studying the influence of temperature on selectivity, oxygen conversion was always above 90%.

Conductivity Measurements

The total conductivities of Me^{n+} (1 at-%)-doped La_2O_3 catalysts were determined by measuring the specific resistance of a catalyst disc with the two-electrode AC method at 1023 K in dependence on the oxygen partial pressure (6, 21). The oxygen partial pressures were varied (0.10, 0.32, 1.00, 3.16, 10.0, 31.6, and 100 kPa).

For preparing the catalyst discs the particles (see above) were first ground and then compacted at 380 MPa into a disc with a diameter of 7 mm and a thickness of about 3 mm; subsequently, the disc was sintered in air for 16 h at 1373 K.

To measure the anionic conductivity only, the sample was sandwiched between two Y_2O_3 (8 mol%)/ZrO_2 discs which were in contact with the Pt-electrodes; hereby, p-type conduction was suppressed (21). The oxygen-anion conductivity was determined at 923, 1023, 1073, and 1123 K.

RESULTS AND DISCUSSION

Oxygen-Anion Conductivity

The oxygen-anion conductivity of the catalysts increased exponentially with temperature. As illustrated in Figs. 1 and 2 the incorporation of lower valent cations (Zn^{2+}, Sr^{2+}) leads to an increase in anion conductivity; for cations of higher valency (Nb^{5+}, Ti^{4+}) the opposite effect was observed. At constant temperature oxygen-anion conductivities of SrO/La_2O_3 mixed oxides increases with a rising SrO content and approaches a maximum value at 3 at-%. Higher dopant concentrations do not result in any significant conductivity change.

The apparent activation energies derived from Figs. 1 and 2 are listed in Table 3. In comparison to undoped La_2O_3, the addition of Ti^{4+} and Nb^{5+} increases the activation energy for oxygen-anion mobility, while it is decreased by the addition of Zn^{2+} or Sr^{2+}. With increasing SrO content the activation energy diminishes from 109 kJ/mol (undoped La_2O_3) to 75 kJ/mol (3 at-% SrO); the activation energy is not significantly changed by further SrO addition up to 20 at-%.

Since oxygen-anion conductivity is directly proportional to the concentration of oxygen lattice vacancies the conductivity change caused by altervalent doping with lower- or higher-valent cations can be attributed to the creation or depletion of anion vacancies. As the formation of solid solutions is favoured when the cations of the host and guest oxide possess similar radii, the incorporation of Sr^{2+} ($r(Sr^{2+}) = 140$ pm) into La_2O_3 ($r(La^{3+}) = 124$ pm) should be easier than of Zn^{2+} ($r(Zn^{2+}) = 88$ pm) (22, 23). It has been reported that the solubility limit of SrO in La_2O_3 is 9 at-% in mixed oxides sintered at 1870 K and increases with further increase of the sintering temperature; maximum solubility of 12.5 at-% has been reached near the melting temperature (about 2570 K) (24, 25). To our knowledge, no information on ZnO/La_2O_3 solid solutions is available in literature. However, it may be assumed that on account of higher solubility more vacancies are formed by addition of SrO, resulting in higher conductivity compared with ZnO/La_2O_3.

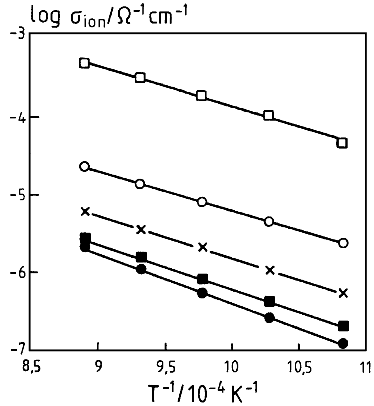

FIG. 1. Arrhenius plot of the dependence of oxygen-anion conductivity on temperature for La_2O_3 and Me^{n+} (1 at-%)/La_2O_3 catalysts. Symbols Me^{n+}: Zn^{2+} (○), Sr^{2+} (□), Ti^{4+} (●), Nb^{5+} (■); La_2O_3 (×).

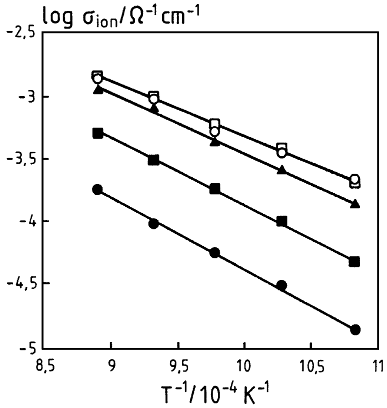

FIG. 2. Arrhenius plot of the dependence of oxygen-anion conductivity on temperature for La_2O_3 and Sr^{2+}/La_2O_3 catalysts. Symbols Sr^{2+} content/at-% : 0.5 (●), 1 (■), 2 (▲), 3 (○), 20 (□).

On increasing the Sr^{2+} content of SrO/La_2O_3 mixed oxides from 1 to 3 at-% the concentration of anion vacancies and, thus, conductivity increases, too (24, 26, 27). A still higher dopant concentration does not result in any further conductivity increase suggesting that the amount of SrO dissolved in the host oxide bulk reaches a limit that cannot be overcome by the preparation conditions applied.

In this context it is worth noting that exposing the catalysts to CO_2 or water vapor leads to a loss in conductivity and also in selectivity; more details have been reported in (21) and further literature has been cited therein.

Total Conductivity of Me^{n+} (1 at-%)-Doped La_2O_3 Catalysts

The logarithm of σ_{total} increases linearly with log P_{O_2} at constant temperature (Fig. 3). The slope of the straight lines

TABLE 3

Apparent Activation Energies E_a of Oxygen-Anion Mobility in Doped La_2O_3 Catalysts

Catalyst	E_a (kJ/mol)
Ti^{4+} (1 at-%)/La_2O_3	123 ± 3
Nb^{5+} (1 at-%)/La_2O_3	110 ± 2
La_2O_3	103 ± 1
Zn^{2+} (1 at-%)/La_2O_3	96 ± 0.5
Sr^{2+} (0.5 at-%)/La_2O_3	99 ± 1
Sr^{2+} (1 at-%)/La_2O_3	95 ± 2
Sr^{2+} (2 at-%)/La_2O_3	91 ± 1
Sr^{2+} (3 at-%)/La_2O_3	75 ± 2
Sr^{2+} (20 at-%)/La_2O_3	77 ± 2

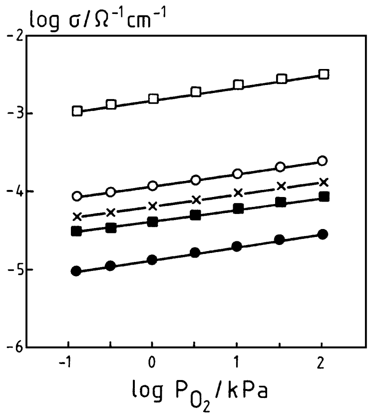

FIG. 3. Total conductivity of La_2O_3 and Me^{n+} (1 at-%)-doped La_2O_3 catalysts at 1023 K as a function of oxygen partial pressure. Symbols Me^{n+}: Zn^{2+} (○), Sr^{2+} (□), Ti^{4+} (●), Nb^{5+} (■); La_2O_3 (×).

is not influenced by the foreign cation. Again, doping La_2O_3 with Sr^{2+} and Zn^{2+} results in an increase in total conductivity while it is diminished by using Ti^{4+} and Nb^{5+} as dopants. Sr^{2+} (1 at-%)/La_2O_3 is more conductive compared to Zn^{2+} (1 at-%)/La_2O.

With increasing oxygen partial pressure the total conductivity increases due to a rise of p-type conductivity which is caused by oxygen adsorption on anion vacancies (Eq. [6])

$$1/2\,O_2(g) + V_O^{\bullet\bullet} \Leftrightarrow O_O^x + 2\,h^{\bullet}. \qquad [6]$$

Assuming that O^{2-} conductivity is independent of oxygen partial pressure the contribution of p-type conductivity to total conductivity can be calculated according to Eq. [7] (28, 29); p-type conductivities of the catalysts at 1023 K and $P_{O_2} = 10$ kPa are listed in Table 4,

$$\sigma_p = \sigma_{total} - \sigma_{ion}. \qquad [7]$$

As indicated by Eq. [6], p-type conductivity is affected by anion vacancy concentration. Therefore, when the concentration of unoccupied O^{2-}-lattice sites is increased by Sr^{2+} or Zn^{2+} doping, not only ionic but also p-type conductivity is increased; addition of Ti^{4+} or Nb^{5+} causes the opposite effect.

TABLE 4

Oxygen-Anion Conductivity σ_{ion} and p-type Conductivity σ_p of La_2O_3 and Me^{n+} (1 at-%)-Doped La_2O_3 Catalysts

Catalyst	$\sigma_{ion}/\Omega^{-1}\,cm^{-1}$	$\sigma_p/\Omega^{-1}\,cm^{-1}$	σ_{ion}/σ_p
Sr^{2+} (1 at-%)/La_2O_3	$2.2 * 10^{-4}$	$2.2 * 10^{-3}$	0.100
Zn^{2+} (1 at-%)/La_2O_3	$8.5 * 10^{-6}$	$1.7 * 10^{-4}$	0.050
La_2O_3	$2.1 * 10^{-6}$	$9.8 * 10^{-5}$	0.021
Nb^{5+} (1 at-%)/La_2O_3	$8.3 * 10^{-7}$	$6.2 * 10^{-5}$	0.013
Ti^{4+} (1 at-%)/La_2O_3	$5.6 * 10^{-7}$	$1.9 * 10^{-5}$	0.029

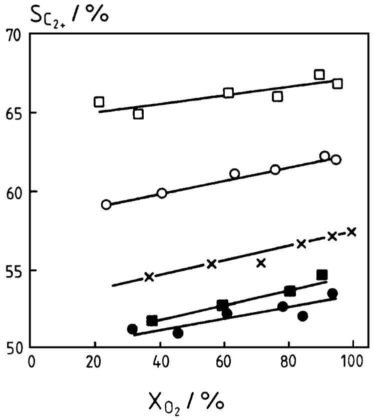

FIG. 4. Dependence of C_{2+} selectivity on oxygen conversion of La_2O_3 and Me^{n+} (1 at-%)-doped La_2O_3 catalysts. (Reaction conditions: T = 1023 K, $P^{\circ}_{CH_4} = 60$ kPa, $P^{\circ}_{O_2} = 6$ kPa, $P^{\circ}_{N_2} = 34$ kPa.) Symbols Me^{n+}: Zn^{2+} (○), Sr^{2+} (□), Ti^{4+} (●), Nb^{5+} (■); La_2O_3 (×).

Catalytic Properties

For La_2O_3 and Me^{n+} (1 at-%)-doped La_2O_3 catalysts ($Me^{n+} = Sr^{2+}$, Zn^{2+}, Ti^{4+}, and Nb^{5+}) the dependence of C_{2+} selectivity on oxygen conversion follows a similar pattern, i.e., the selectivity increases with increasing conversion as shown in Fig. 4, (this may be ascribed to the positive effect of low oxygen concentration at high degrees of conversion dominating the negative effect of high O_2 concentration at low conversion).

At constant conversion ($X_{O_2} > 90\%$) C_{2+} selectivity is enhanced by high temperatures and reaches a maximum at 1123 K (see Fig. 5). It is evident that at comparable reaction conditions the selectivity is significantly increased by incorporating Zn^{2+} or Sr^{2+} into La_2O_3, whereas it is decreased substantially by doping with Ti^{4+} and Nb^{5+}.

C_{2+} selectivity as a function of the Sr^{2+} content passes through a maximum at 1 at-% Sr^{2+}. As depicted in Fig. 6,

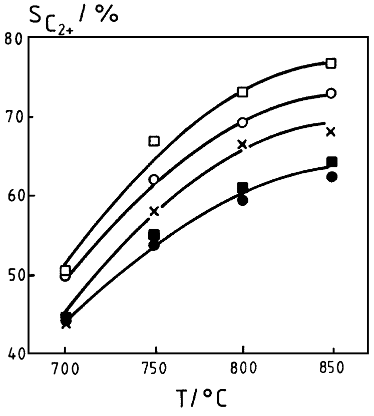

FIG. 5. C_{2+} selectivity of La_2O_3 and Me^{n+} (1 at-%)-doped La_2O_3 catalysts as a function of temperature. (Reaction conditions: $P^{\circ}_{CH_4} = 60$ kPa, $P^{\circ}_{O_2} = 6$ kPa, $P^{\circ}_{N_2} = 34$ kPa, $X_{O_2} > 90\%$.) Symbols Me^{n+}: Zn^{2+} (○), Sr^{2+} (□), Ti^{4+} (●), Nb^{5+} (■); La_2O_3 (×).

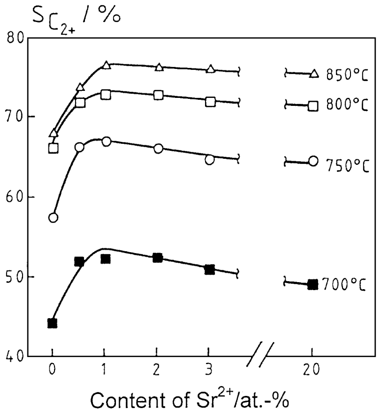

FIG. 6. Dependence of C_{2+} selectivity of Sr^{2+}-doped La_2O_3 catalysts on temperature. (Reaction conditions: $P^{\circ}_{CH_4} = 60$ kPa, $P^{\circ}_{O_2} = 6$ kPa, $P^{\circ}_{N_2} = 34$ kPa, $X_{O_2} > 90\%$.)

C_{2+} selectivity decreases slightly when increasing the Sr^{2+} content from 1 to 20 at-%.

Correlation between Oxygen-Anion Conductivity and C_{2+} Selectivity

The marked differences in selectivity of undoped La_2O_3 and Me^{n+} (1 at-%)-doped La_2O_3 catalysts are certainly not due to their textural properties since their specific surface areas do not differ significantly (see catalyst preparation). Also, the beneficial effect of incorporating lower valent cations cannot be simply ascribed to the change of surface basicity or acidity, because both the addition of basic SrO or of acidic ZnO (compared to La_2O_3 (30)) result in an enhancement of C_{2+} selectivity.

The promoting effect of various dopants on C_{2+} selectivity appears to be most likely related to a change of oxygen-anion conductivity. For corroborating this relationship C_{2+} selectivities of various catalysts ($X_{O_2} > 90\%$) were plotted as a function of oxygen-anion conductivity in Fig. 7 for different temperatures. As a most intriguing feature this plot manifests that oxygen-anion conductivity is obviously the overwhelming catalyst property which affects C_{2+} selectivity, i.e., the higher oxygen-anion conductivity the higher C_{2+} selectivity.

The positive effect of a high oxygen-anion conductivity may be rationalized in the following manner: a high concentration of anion vacancies favours the adsorption of gaseous oxygen and its subsequent transformation into lattice oxygen. This is also confirmed by the increase in p-type conductivity reflecting the higher activity with respect to oxygen take-up. As a consequence nonselective surface reactions of methyl species and C_2 hydrocarbons with weakly adsorbed oxygen species are suppressed. However, the temperature dependence of C_{2+} selectivity cannot be explained by the temperature dependence of O^{2-} conductivity alone; with increasing temperature the C_{2+} selectivity increase is more pronounced than that of conductivity and approaches a maximum. The activation energies of the selective ($CH_4 \rightarrow C_2H_6 + C_2H_4$) and nonselective steps ($CH_4 \rightarrow CO_x$) of the OCM reaction over a SrO (1 wt-%)-doped La_2O_3 catalyst were found to be 154 $kJmol^{-1}$ and 100 $kJmol^{-1}$, respectively (31). In contrast, the activation energy of oxygen-anion conductivity in Sr (1 at-%)-doped La_2O_3 amounts only to 96 $kJmol^{-1}$, explaining formally the stronger temperature dependence of C_{2+} selectivity. According to Lunsford (1, 32) the higher activation energy of the selective reaction step can be ascribed to the regeneration of anion vacancies on the catalyst surface by dehydration, which is promoted by higher reaction temperatures. Therefore, the positive influence of temperature on C_{2+} selectivity is due to an increasing oxygen-anion mobility and an enhanced dehydration, resulting in a higher concentration of oxygen-anion vacancies on the surface. This suggests that selective catalysts require a low activation energy of oxygen-anion conductivity in order to attain high oxygen mobilities at low temperatures.

From the above results and the respective discussion it might be concluded that changes in the foreign-cation content should affect conductivity and thus, C_{2+} selectivity. However, whereas anionic conductivity of SrO-doped La_2O_3 increases with increasing SrO content C_{2+} selectivity passes through a maximum at 1.0 at-% Sr (see Figs. 2 and 6). The question arises how this selectivity maximum may be explained. XPS investigations revealed that strontium is strongly enriched in the near surface layers of the Sr-doped La_2O_3 catalysts (see Table 2). Since the surface concentration of SrO exceeded the equilibrium solubility there appears to be a phase of unsolved SrO on the surface of a high-conductivity SrO–La_2O_3 solid solution. Although SrO is known to be an oxygen-anion insulator its enrichment on the crystalline surface in the concentration range investigated has no obvious influence on the ionic conductivity of

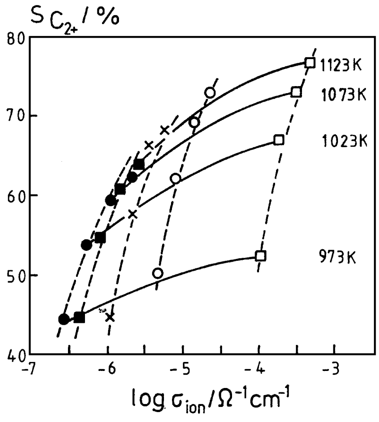

FIG. 7. C_{2+} selectivity of La_2O_3 and Me^{n+} (1 at-%)/La_2O_3 catalysts in dependence on oxygen-anion conductivity. (Reaction conditions: $P^{\circ}_{CH_4} = 60$ kPa, $P^{\circ}_{O_2} = 6$ kPa, $P^{\circ}_{N_2} = 34$ kPa, $X_{O_2} > 90\%$.) Symbols Me^{n+} : Zn^{2+} (○), Sr^{2+} (□), Ti^{4+} (●), Nb^{5+} (■); La_2O_3 (×).

the catalyst; this fact was also observed by Deportes and co-workers (33). One might assume that there is a compensating effect between bulk and surface conductivity; i.e., whereas conductivity in the bulk is increased with increasing SrO content, conductivity in the near-surface region decreases due to a low-conductivity marginal layer of segregated SrO, as has been discussed already for CaO/CeO_2 solid solutions (34).

According to the above reasoning the catalytic performance can be explained as follows: The increasing coverage of the catalyst surface by insulating SrO inhibits the diffusional exchange of oxygen-anions, as well as vacancies between surface and bulk of the catalyst. Consequently, the concentration of unoccupied oxygen lattice sites on the surface decreases, although the bulk defect concentration increases, leading to higher oxygen-anion conductivity. By blocking the oxygen anion vacancies, the transformation of weakly adsorbed oxygen species into lattice oxygen is restrained markedly, resulting in a selectivity decrease as compared to the maximum.

CONCLUSIONS

Assuming a dynamic equilibrium between the concentration of oxygen anion vacancies in the bulk and on the surface of the solid catalyst the incorporation of adsorbed oxygen in the catalyst is favoured by a high oxygen-anion conductivity. Hence, the coverage of the surface with electrophilic oxygen species is reduced in favour of nucleophilic species. The correlation between the anionic conductivity as a bulk property and the catalytic behaviour as a property of the surface is only possible as long as the composition of the bulk and the outmost surface are similar. With increasing strontium content in a SrO-doped La_2O_3 catalyst leading to SrO segregation and its enrichment on the surface the diffusive exchange of oxygen anions and anionic vacancies between the bulk and the outer surface is limited. Hereby, the adsorption of gaseous oxygen and the transformation of adsorbed oxygen species into lattice oxygen is restrained, resulting in a selectivity loss.

ACKNOWLEDGMENT

Financial support by the European Union and Fonds der chemisch en Industrie has been greatly appreciated.

REFERENCES

1. Ito, T., and Lunsford, J. H., *Nature*, 314 (1985).
2. Campbell, K. D., Zhang, H., and Lunsford, J. H., *J. Phys. Chem.* **92**, 750 (1988).
3. Sokolovskii, V. D., *React. Kinet Catal. Lett.* **35**, 337 (1987).
4. Sokolovskii, V. D., Aliev, S. M., Buyevskaya, O. V., and Davydov, A. A., *Catal. Today* **4**, 293 (1989).
5. Kaliaguine, S. L., Shelimov, B. N., and Kazansky, V. B., *J. Catal.* **55**, 384 (1978).
6. Zhang, Z., Verykios, X. E., and Baerns, M., *Catal. Rev.-Sci. Eng.* **36**, 507 (1994).
7. Anshits, A. G., Voskresenskaya, E. N., Kondradenko, E. V., and Maksimov, N. G., *Catal. Today* **24**, 217 (1995).
8. Ying-Li, B., Li-Tao, L., and Kai-Li, Z., *Catal. Today* **24**, 245 (1995).
9. Bielanski, A., and Haber, J., *Catal. Rev.-Sci. Eng.* **19**, 1 (1979).
10. Bielanski, A., and Haber, J., *in* "Oxygen in Catalysis," p. 150, Dekker, New York, 1991.
11. Che, M., and Tench, A. I., *Adv. Catal.* **31**, 77 (1982).
12. Che, M., and Tench, A. I., *Adv. Catal.* **32**, 1 (1983).
13. Peil, K. P., Goodwin, J. G., and Marcelin, G., *J. Phys. Chem.* **93**, 5977 (1989).
14. Peil, K. P., Goodwin, J. G., and Marcelin, G., *J. Catal.* **131**, 143 (1991).
15. Kalenik, Z., and Wolf, E. E., *Prep.-ACS, Div. Petro. Chem.* **37**, 1 (1992).
16. Ekstrom, A., and Lapszewicz, J. A., *J. Am. Chem. Soc.* **110**, 5226 (1988).
17. Kudo, T., and Fueki, K., *in* "Solid State Ionics," p. 70, Verlag Chemie, Weinheim, 1990.
18. Dubois, J. L., and Cameron, C. J., *Appl. Catal.* **67**, 49 (1990).
19. Taylor, R. P., and Schrader, G. L., *Ind. Eng. Chem. Res.* **30**, 1016 (1991).
20. Deboy, J. M., and Hicks, R. F., *J. Chem. Soc., Chem. Commun.*, 982 (1988).
21. Borchert, H., Doctoral thesis, Ruhr-University Bochum, Germany, 1993.
22. Shannon, R. D., and Prewitt, C. T., *Acta Crystallogr.* **B25**, 925 (1969).
23. Shannon, R. D., *Acta Crystallogr.* **A32**, 751 (1976).
24. Milne, S. J., Brock, R. J., and Zhen, Y. S., *Br. Ceram. Proc. (Electroceramics)* **41**, 243 (1989).
25. Queyroux, F., *Rev. Hautes Temp. Refract.* **6**, 111 (1969).
26. Zhen, Y. S., Milne, S. J., and Brook, R. J., *in* "High Tech Ceramics" (P. Vincenzini, Ed.), p. 1989, Elsevier, Amsterdam, 1987.
27. Etsell, T. H., and Felngas, S. N., *J. Electrochem. Soc.* **116**, 771 (1969).
28. Kiukkola, K., and Wagner, C., *J. Electrochem. Soc.* **104**, 379 (1957).
29. Foex, M., and Traverse, J. P., *Bull. Soc. France Mineral. Crist.* **89**, 184 (1966).
30. Auroux, A., and Gervasini, A., *J. Phys. Chem.* **94**, 6371 (1990).
31. Deboy, J. M., and Hicks, R. F., *J. Catal.* **113**, 517 (1988).
32. Campbell, K. D., and Lunsford, J. H., *J. Phys. Chem.* **86**, 2760 (1982).
33. Vanbaelinghem, F., Pelloux, A., and Deportes, C., *J. Appl. Electrochem.* **6**, 67 (1976).
34. El Adham, K., and Hamman, H., *Solid State Ionics* **9, 10**, 905 (1983).